British Journal of Pharmacology (2008) 153, 110–123
 0007–1188/08 $30.00
www.brjpharmacol.org

RESEARCH PAPER

Electromechanical characterization of cinnamophilin, a natural thromboxane A_2 receptor antagonist with anti-arrhythmic activity, in guinea-pig heart

G-J Chang[1], M-J Su[2], T-S Wu[3,4], W-P Chen[2] and C-M Kuo[1]

[1]*Graduate Institute of Clinical Medicinal Sciences, College of Medicine, Chang Gung University, Tao-Yuan, Taiwan;* [2]*Pharmacological Institute, College of Medicine, National Taiwan University, Taipei, Taiwan;* [3]*Department of Chemistry, National Cheng Kung University, Tainan, Taiwan and* [4]*National Research Institute of Chinese Medicine, Taipei, Taiwan*

Background and purpose: Cinnamophilin, a thromboxane A_2 receptor antagonist, has been identified as a prominent anti-arrhythmic agent in rat heart. This study aimed to determine its electromechanical and anti-arrhythmic effects in guinea-pig hearts.

Experimental approach: Microelectrodes were used to study action potentials in ventricular papillary muscles. Fluo-3 fluorimetric ratio and whole-cell voltage-clamp techniques were used to record calcium transients and membrane currents in single ventricular myocytes, respectively. Intracardiac electrocardiograms were obtained and the anti-arrhythmic efficacy was determined from isolated perfused hearts.

Key results: In papillary muscles, cinnamophilin decreased the maximal rate of upstroke (V_{max}) and duration of action potential, and reduced the contractile force. In single ventricular myocytes, cinnamophilin reduced Ca^{2+} transient amplitude. Cinnamophilin decreased the L-type Ca^{2+} current ($I_{Ca,L}$)($IC_{50} = 7.5$ μM) with use-dependency, induced a negative shift of the voltage-dependent inactivation and retarded recovery from inactivation. Cinnamophilin also decreased the Na^+ current (I_{Na}) ($IC_{50} = 2.7$ μM) and to a lesser extent, the delayed outward (I_K), inward rectifier (I_{K1}), and ATP-sensitive ($I_{K,ATP}$) K^+ currents. In isolated perfused hearts, cinnamophilin prolonged the AV nodal conduction interval and Wenckebach cycle length and the refractory periods of the AV node, His-Purkinje system and ventricle, while shortening the ventricular repolarization time. Additionally, cinnamophilin reduced the occurrence of reperfusion-induced ventricular fibrillation.

Conclusions and implications: These results suggest that the promising anti-arrhythmic effect and the changes in the electromechanical function induced by cinnamophilin in guinea-pig heart can be chiefly accounted for by inhibition of $I_{Ca,L}$ and I_{Na}.
British Journal of Pharmacology (2008) **153**, 110–123; doi:10.1038/sj.bjp.0707541; published online 29 October 2007

Keywords: cinnamophilin; action potential; calcium transient; voltage clamp; calcium current; sodium current; potassium current; cardiomyocytes; conduction system; cardiac arrhythmias

Abbreviations: AERP, atrial effective refractory period; AH, atrio-His bundle conduction interval; APA, action potential amplitude; $APD_{25,\ 50,\ 90}$, action potential duration measured at 25, 50 and 90% repolarization; AVNERP, AV nodal effective refractory period; BCL, basic cycle length; *G*, conductance; HPFRP, His-Purkinje system functional refractory period; HV, His-ventricular conduction interval; $I_{Ca,L}$, L-type Ca^{2+} inward current; I_K, delayed rectifier K^+ current; I_{K1}, inward rectifier K^+ current; $I_{K,ATP}$, ATP-sensitive K^+ current; I_{Na}, Na^+ inward current; I_{to}, transient outward K^+ current; K_{ATP}, ATP-sensitive K^+ channel; *k*, slope factor; RMP, resting membrane potential; SA, sinoatrial conduction interval; SOD, superoxide dismutase; TXA_2, thromboxane A_2; τ_f and τ_s, fast and slow time constant; VERP, ventricular effective refractory period; VF, ventricular fibrillation; V_h, half-maximal potential; V_{max}, maximal upstroke velocity of action potential; VRT, ventricular repolarization time; WCL, Wenckebach cycle length

Introduction

Cinnamophilin is a novel lignan compound isolated from the plant *Cinnamomum philippinense* (Wu *et al.*, 1994). Previous *in vitro* and *in vivo* studies have demonstrated that cinnamophilin possesses both thromboxane synthase inhibitory and thromboxane A_2 (TXA_2) receptor antagonizing

Correspondence: Professor G-J Chang, Graduate Institute of Clinical Medicinal Sciences, College of Medicine, Chang Gung University, 259 Wen-Hwa 1st Road, Kwei-Shan, Tao-Yuan 333, Taiwan.
E-mail: gjchang@mail.cgu.edu.tw
Received 24 July 2007; revised 5 September 2007; accepted 20 September 2007; published online 29 October 2007

properties (Yu *et al*., 1994a, b). The same study has also shown that this agent relaxed isolated rat thoracic aorta mediated partially by the blockade of voltage-dependent Ca^{2+} channels (Yu *et al*., 1994a). Moreover, cinnamophilin was reported to protect ischaemic skeletal muscle from the reperfusion injury in rats (Cheng and Chang, 1995) and to act as a novel antioxidant and cytoprotectant against oxidative damage (Hsiao *et al*., 2001). In a recent study performed in isolated Langendorff-perfused rat heart, cinnamophilin was effective in the reduction of the coronary artery ligation/reperfusion-induced arrhythmias (Su *et al*., 1999). This profile of activity may be attributed to its electrophysiological actions such as blockade of the transient outward K^+ (I_{to}), Na^+ and Ca^{2+} channels (Su *et al*., 1999).

The cardiac action potential waveforms differ between animal species, owing to differences in ion channel expression (Nerbonne and Kass, 2005). Evidence indicates that cinnamophilin caused a significant prolongation of rat cardiac action potential (Su *et al*., 1999) which displays a prominent phase 1 repolarization and a brief plateau occurs at more negative potentials (Josephson *et al*., 1984). The class III anti-arrhythmic agent-like property is mainly due to the blockade of the I_{to} (Su *et al*., 1999) which is the most important repolarizing current in rat heart (Josephson *et al*., 1984). Nevertheless, whether cinnamophilin could also display class III-like effects in cardiac preparations from other commonly studied mammalian species (for example, guinea-pig or rabbit) with long-lasting action potential plateau and functionally expressed delayed rectifier K^+ current (I_K) channel (Hume and Uehara, 1985; Varró *et al*., 1993) as in human heart (Li *et al*., 1996) are yet to be determined. In the present study, therefore, we characterized the electromechanical and anti-arrhythmic profiles of cinnamophilin in guinea-pig heart preparations. Our results indicate that cinnamophilin predominantly blocks L-type Ca^{2+} inward current ($I_{Ca,L}$) and Na^+ inward current (I_{Na}) in guinea-pig cardiomyocytes. These effects may contribute to the modification of the electromechanical properties and anti-arrhythmic action in guinea-pig heart preparations and also, a marked difference on action potential waveforms in contrast to that previously reported in rat hearts.

Materials and methods

Animal procedures

The investigation was approved by the animal use committee of our institution and conformed to the *Guide for the Care and Use of Laboratory Animals* (NIH publication no. 85-23, revised 1996). Adult male Hartley guinea-pigs weighing 250–350 g were anaesthetized with sodium pentobarbital (50 mg kg^{-1}) and given heparin (300 U kg^{-1}) by i.p. injection and killed by cervical dislocation.

Electromechanical recordings

The guinea-pig heart was quickly excised via a thoracotomy. Right ventricular papillary muscles (0.5–1 mm in diameter and 3–5 mm in length) were dissected free and mounted in a tissue chamber and superfused at a rate of 20 ml min^{-1} with an oxygenated (95% O_2 and 5% CO_2) normal Tyrode solution at 37 °C (Chang *et al*., 2006). The muscles were stimulated by 1 ms and 1.5 times-threshold strength pulses at 1 Hz. Transmembrane potentials were recorded with a glass microelectrode filled with 3 M KCl (tip resistance: 15–25 MΩ), which was connected to the input stage of an Axoclamp 2B amplifier (Molecular Devices, Sunnyvale, CA, USA). The contractile force was recorded by a Quad bridge amplifier (ADInstruments Pty Ltd, Castle Hill, Australia). Signals were digitized at 10 kHz using a PowerLab/4sp digitizer and stored on an online computer and analysed by Chart4.0.2 software (ADInstruments) thereafter.

Measurement of the intracellular Ca^{2+} transients

Single ventricular myocytes from adult guinea-pigs were enzymatically dissociated as described previously (Chang *et al*., 2006). Ventricular myocytes were loaded with fluo-3 by incubating with 0.5 mM Ca^{2+} HEPES-buffered Tyrode solution containing 5 μM fluo-3/acetoxymethyl ester (fluo-3/AM) and Pluronic F-127 (2%) for 30 min at room temperature. After washing out the excess fluo-3/AM, cells were then transferred to 1.8 mM Ca^{2+}-containing solution for at least 30 min before beginning the experiments. Myocytes were electrically stimulated by 2 ms and twice-threshold pulses at 1 Hz. Fluorescent changes were detected by a Zeiss LSM-510 laser scanning confocal system (Carl Zeiss, MicroImaging GmbH, Jena, Germany). Fluo-3 was excited with a 488-nm argon laser, and fluorescence emission was measured using a 505–550 nm band-pass filter and acquired by image acquisition system every 1 min. The intracellular Ca^{2+} transients are reported as relative fluorescence, or F/F_0, where F is the fluorescence signal and F_0 is the resting fluorescence recorded at the start of the experiment.

Whole cell recording

Patch-clamp experiments were performed at room temperature (25–27 °C). Ventricular myocytes were bathed in a HEPES-buffered Tyrode solution. The conventional whole-cell patch-clamp technique was used to record Na^+ and K^+ currents, while the amphotericin B-perforated patch technique was employed to record Ca^{2+} current. Patch electrodes were pulled from glass capillaries (outer diameter (o.d.): 1.5 mm, inner diameter (i.d.): 1.0 mm; A-M Systems, Carlsborg, WA, USA) and fire-polished to give a pipette resistance of 2–5 MΩ for conventional whole-cell clamp and 1–2 MΩ for perforated patch technique when filled with the pipette solutions. Membrane currents were recorded using the Axopatch 200B amplifier (Molecular Devices) linked to a Digidata 1320A A/D converter (Molecular Devices). Electrode junction potentials (5–10 mV) were nulled before suction of the cell. In the perforated patch method, the access resistance decreased to <10 MΩ within 15–30 min after seal formation. The total series resistance (R_s) was estimated from the cell capacitance and capacitance current decay and was about 4–6 MΩ. This was reduced to 1–2 MΩ with 60–80% compensation. Capacitance of the cell was measured by calculating the total charge movement of the capacitative transient in response to a 5-mV hyperpolarizing pulse and was 130.3 ± 5.3 pF ($n=36$).

During measurement of K^+ currents, Ca^{2+} currents were blocked by addition of 5 μM nifedipine to the bathing solution, and Na^+ currents were voltage-inactivated by maintaining the holding potential at –40 mV. During measurement of ATP-sensitive K^+ current ($I_{K,ATP}$), current–voltage (*I–V*) relations were recorded by applying voltage ramp pulses. The current recorded at 0-mV clamp potential was evaluated. At this voltage, most of the time- and voltage-dependent currents are very small. $I_{Ca,L}$ was recorded using tetrodotoxin (30 μM) and CsCl (2 mM)-containing bath solution and Cs^+ pipette solution designed to minimize currents through Na^+ and K^+ channels. In addition, a prepulse potential of –40 mV was used to inactivate Na^+ and T-type Ca^{2+} channels. To lower the maximal amplitude of Na^+ currents, I_{Na} was studied in a low Na^+ Tyrode solution ($[Na^+] = 54$ mM, with NaCl replaced by *N*-methyl-D-glucamine) and dialysis of the cell with Na^+-containing (10 mM) Cs^+ pipette solution. Since the peak I_{Na} measured in this study was <7 nA, the voltage errors attributed to uncompensated R_s ($I_{Na} \times R_s$) would be <10 mV.

Data acquisition and analysis

Recordings were filtered at 10 kHz, acquired at 100 kHz, and stored and analysed using pClamp8.0.2 software (Molecular Devices). I_K tail current ($I_{K,tail}$) was measured as the difference from the steady-state holding current level to the peak tail current amplitude. Inward rectifier K^+ current (I_{K1}) was measured as the current amplitude at the end of the voltage step. Both $I_{Ca,L}$ and I_{Na} were measured as the peak inward current amplitudes. I_K rundown was prominent during the initial 5–8 min access of the patch pipette to the interior of the cell with no significant change over 30 min thereafter. When $I_{K,tail}$ (evoked at $+60$ mV) was normalized to the value at 1 min after disruption of the membrane patch, it decreased to 86 ± 4, 77 ± 3, 75 ± 3, 71 ± 3 and 70 ± 4% ($n = 12$) during the subsequent 3, 6, 9, 15 and 21 min, respectively. Therefore, the trace at the end of the 10 min control period was taken as the control trace. The rundown of $I_{Ca,L}$ was very small during the following 30–40 min under the stable perforated patch conditions. When $I_{Ca,L}$ (at 0 mV) was normalized to the first record after formation of stable perforated patch, it changed to 102 ± 3, 98 ± 2, 96 ± 4 and 97 ± 4% ($n = 11$) during the subsequent 3, 9, 15 and 21 min, respectively. The Ca^{2+}-conductance (G) was calculated from the equation $G = I_{Ca,L}/(V_m - V_{rev})$, where $I_{Ca,L}$ is the current amplitudes of Ca^{2+} channel at given membrane potential (V_m) and V_{rev} is the reversal potential ($+60$ mV). G_{max} is the maximal Ca^{2+} conductance (calculated at potentials above $+10$ mV). The ratio G/G_{max} was plotted against the V_m and fitted to the Boltzmann equation. Concentration–response curves were fitted by the equation $E = E_{max}/[1 + (IC_{50}/C)^{n_H}]$, where E is the effect at concentration C, E_{max} is maximal effect, IC_{50} is the concentration for half-maximal block and n_H is the Hill coefficient.

Intracardiac ECG recording

The guinea-pig heart was excised via a thoracotomy and the aorta was retrogradely perfused with normal Tyrode solution. A bipolar tungsten spring-soldered silver electrode was placed near the apex of the triangle of Koch to record the His bundle electrogram, while the other silver electrode was placed on the ventricular apex to record ventricular signals. To pace the atrium and ventricle, one electrode was placed on the right atrium and the other one was placed on the right ventricular apex, respectively. A programmable stimulator (DTU 215, Fischer imaging Co., Denver, CO, USA) was used to deliver pacing stimulus (twice-threshold strength, 1 ms duration). The signals were continuously monitored and recorded on a chart recorder (WindowGraf, Gould Inc., Cleveland, OH, USA) and digitized using an A/D converter (IWX/214, iWorx, Dover, NH, USA) and stored on an online computer. Electrophysiological studies were performed according to the standard methods described previously (Chang *et al.*, 2002, 2006). An average of four stable cycle lengths of spontaneous heartbeats was taken as the basic cycle length (BCL). The right atrium was then paced at a constant rate that was slightly faster than the spontaneous heart rate, and the intra-atrial (sinoatrial conduction interval (SA)), AV nodal (atrio-His bundle conduction interval (AH)) and His-ventricular (HV) conduction intervals, and ventricular repolarization time (VRT) were measured. Incremental right atrial pacing rates were used to determine the Wenckebach cycle length (WCL), at which the 1:1 AV conduction was lost. Atrial extrastimulation (S_2) was performed to obtain the refractory periods of the atria, AV node and the His-Purkinje system. The ventricular effective refractory period (VERP) was similarly determined by a ventricular extrastimulation study protocol.

Global ischaemia/reperfusion-induced arrhythmias

Details of this methodology have been described previously (Chang *et al.*, 2006). The isolated guinea-pig heart was retrogradely perfused through the aorta with normal Tyrode solution at a constant pressure. Following a 10-min equilibration period, the hearts were administered drug or vehicle for 10 min. After this pre-ischaemic period, the aortic cannula was clamped to institute global no-flow ischaemia. The electrograms were recorded from a low atrial and a ventricular recording electrode. After 30-min ischaemia, the aortic cannula was unclamped to permit reperfusion and the incidence and mean duration of ventricular arrhythmias were recorded and analysed. The drug or vehicle level was maintained throughout the ischaemia and reperfusion time course.

Solutions

The normal Tyrode solution contained (in mM): NaCl 137, KCl 5.4, $MgCl_2$ 1.1, $NaHCO_3$ 11.9, NaH_2PO_4 0.33, $CaCl_2$ 1.8 and dextrose 11. The HEPES-buffered Tyrode solution contained (in mM): NaCl 137, KCl 5.4, KH_2PO_4 1.2, $MgSO_4$ 1.22, $CaCl_2$ 1.8, dextrose 22 and HEPES 6.0, titrated to pH 7.4 with NaOH. The pipette solution contained (in mM): KCl 20, aspartic acid 120, $MgCl_2$ 1.0, K_2ATP 5.0, Na_2 phosphocreatine 5.0, NaGTP 0.2, EGTA 5.0 and HEPES 10, adjusted to pH 7.2 with KOH. The Cs^+-containing pipette solution for $I_{Ca,L}$

recording contained (in mM): CsCl 130, tetraethylammonium chloride (TEA Cl) 15, $MgCl_2$ 5.0 and HEPES 10, adjusted to pH 7.2 with CsOH. The Cs^+-containing pipette solution for I_{Na} recording contained (in mM): CsCl 130, NaCl 10, EGTA 5.0, TEA Cl 15, dextrose 5.0 and HEPES 10, adjusted to pH 7.2 with CsOH.

Statistics

Data are expressed as the means ± s.e.mean. Within-group comparisons among control and post-treatment dosage were made using an ANOVA for repeated measures with Dunnett's *t*-test for multiple comparisons. Incidences of arrhythmias were compared by a χ^2 procedure followed by pairwise comparison by use of a Fisher's exact test. $P<0.05$ was considered to be statistically significant.

Materials

Cinnamophilin was isolated from the plant *Cinnamomum philippinense* (Wu *et al*., 1994) and its purity was estimated to be >99% on the basis of ^{1}H-NMR (400–200 MHz), IR and MS (70 eV). Most of the drugs were purchased from Sigma-Aldrich Co. (St Louis, MO, USA) except fluo-3/AM and Pluronic F127 were purchased from Molecular Probes (Eugene, OR, USA). Cinnamophilin, nifedipine, fluo-3/AM, Pluronic F127, diltiazem, ozagrel, SQ29548, cromakalim, glibenclamide and amphotericin B were dissolved in dimethylsulphoxide (DMSO). Other drugs were dissolved in physiological saline before the start of the experiment. Amphotericin B (100 mg ml^{-1}) was freshly prepared in DMSO and then added at a final concentration of 240 μg ml^{-1} to the Cs^+-containing pipette solution. In control experiments, DMSO (up to 0.1%) alone produced no significant effect on electrophysiological and mechanical parameters of the heart preparations.

Results

Electromechanical effects of cinnamophilin on ventricular papillary muscles

Figure 1a and Table 1 show that cinnamophilin shortened the duration of action potential measured at 25, 50 and 90% repolarization ($APD_{25,\ 50,\ 90}$) and decreased both the maximal upstroke velocity of action potential (V_{max}) and contractile force of guinea-pig ventricular papillary muscle concentration-dependently. Cinnamophilin had no effect on the resting membrane potential and action potential amplitude. The effect on action potential and contractility reached a steady state in less than 8–10 min and partially reversed following about 60 min washout by drug-free solution. For comparison, the effect of a typical Ca^{2+} channel blocker diltiazem was also examined. Similar changes in action potential configuration and contractile force were produced by diltiazem, although this drug induced no significant decrease in V_{max} (Figure 1b and Table 1).

Effects of cinnamophilin on intracellular Ca^{2+} transients

Figure 2 shows representative tracings of the normalized fluo-3 fluorescence signals (F/F_0) at the control levels and 5 min each after exposure to 1, 3 and 10 μM cinnamophilin. It can be clearly seen that cinnamophilin produced a concentration-dependent decrease in the amplitude of the intracellular Ca^{2+} transient. The mean decrease in F/F_0 was 15 ± 6, 38 ± 10 and 60 ± 7% ($n=4$) at 1, 3 and 10 μM, respectively.

Effects of cinnamophilin on $I_{Ca,L}$

$I_{Ca,L}$ was elicited by a depolarizing pulse to 0 mV from a prepulse of –40 mV (holding potential = –80 mV) in ventricular cells at 0.1 Hz. Cinnamophilin gradually inhibited $I_{Ca,L}$

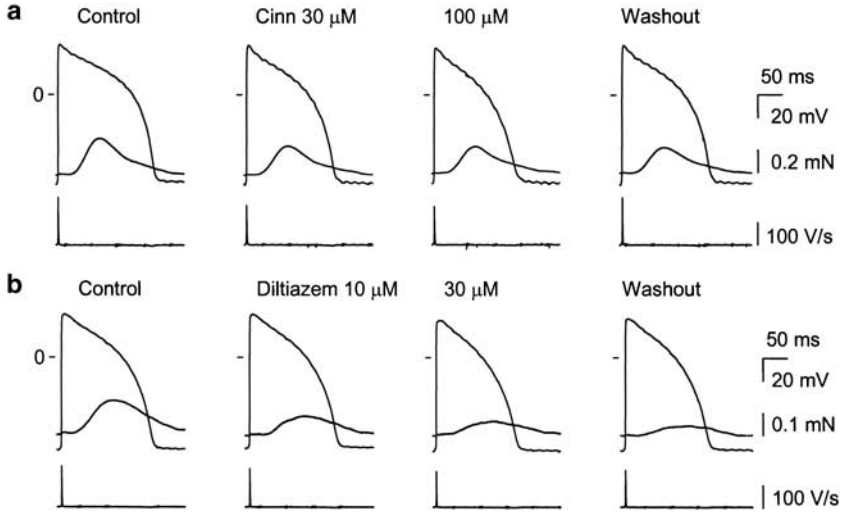

Figure 1 Original records of transmembrane action potential and isometric contraction in guinea-pig papillary muscles driven at 1 Hz before and following cumulative exposures to 30 and 100 μM cinnamophilin (Cinn) (**a**) or 10 and 30 μM diltiazem (**b**), and after 60 min washout. Traces from top to bottom in each panel show contractile force, action potential and V_{max}, respectively. Records were obtained at the end of a 20-min exposure time to each concentration of drug. V_{max}, maximal upstroke velocity of action potential.

Table 1 Effects of cinnamophilin (Cinn) (A) and diltiazem (B) on the action potential parameters and contractile force in guinea-pig ventricular papillary muscles driven at 1 Hz

	RMP (mV)	*APA (mV)*	*V_{max} (V s^{-1})*	*APD_{25} (ms)*	*APD_{50} (ms)*	*APD_{90} (ms)*	*CF (%)*
A ($n=10$)							
Control	–85.5 ± 0.9	122.3 ± 1.4	196.4 ± 6.6	95.6 ± 4.8	148.3 ± 4.7	180.6 ± 4.0	100.0 ± 0.0
Cinn							
10 μM	–83.2 ± 1.5	120.7 ± 2.0	181.4 ± 9.0	86.1 ± 5.6	137.5 ± 5.2	171.5 ± 4.3	86.9 ± 4.6
30 μM	–82.1 ± 2.0	119.8 ± 2.2	173.7 ± 7.3	80.4 ± 4.8	129.8 ± 4.6	166.7 ± 3.9	70.6 ± 6.9*
100 μM	–82.4 ± 1.3	118.8 ± 2.4	162.0 ± 6.7*	72.6 ± 4.5*	120.5 ± 4.7**	163.3 ± 4.0*	66.0 ± 9.3**
Washout	–83.0 ± 2.2	121.2 ± 1.0	184.1 ± 10.2	81.1 ± 5.0	130.5 ± 4.1	169.2 ± 3.1	69.9 ± 8.9*
B ($n=7$)							
Control	–85.8 ± 0.8	123.6 ± 0.7	182.5 ± 13.1	100.0 ± 4.3	148.6 ± 5.2	179.9 ± 6.2	100.0 ± 0.0
Diltiazem							
3 μM	–83.8 ± 0.9	123.3 ± 0.6	182.1 ± 16.8	92.9 ± 3.6	141.6 ± 3.1	173.9 ± 3.9	81.8 ± 6.2
10 μM	–83.9 ± 1.7	121.6 ± 0.7	174.2 ± 15.3	86.2 ± 3.6	133.3 ± 2.9	166.2 ± 3.5	65.0 ± 4.7**
30 μM	–84.2 ± 1.9	119.2 ± 0.8**	159.9 ± 15.5	73.2 ± 4.5**	117.1 ± 5.2**	152.0 ± 5.4**	46.5 ± 3.2#
Washout	–86.6 ± 1.1	121.0 ± 0.5	170.8 ± 13.0	86.9 ± 6.6	136.0 ± 7.0	167.3 ± 7.5	45.5 ± 1.9#

Abbreviations: APA, action potential amplitude; APD_{25}, APD_{50}, and APD_{90}, action potential duration measured at 25, 50, and 90% repolarization, respectively; CF, contractile force; RMP, resting membrame potential; V_{max}, maximal upstroke velocity of action potential.
Values are means ± s.e.mean.
*$P<0.05$, **$P<0.01$, and #$P<0.001$ compared to respective control value by ANOVA, followed by Dunnett's *t*-test for multiple comparisons.
Control value of CF are 0.22 ± 0.06 mN ($n=10$) and 0.14 ± 0.04 mN ($n=7$) in cinnamophilin and diltiazem group, respectively.

and the effect reached a steady-state level within 5 min (Figures 3a and b). Partial recovery of $I_{Ca,L}$ was observed after 5 min of drug washout. Diltiazem also produced a potent inhibitory effect on $I_{Ca,L}$ (figure not shown). The concentration–response relationships for the inhibition of $I_{Ca,L}$ by cinnamophilin and diltiazem are shown in Figure 3c. From these data an IC_{50} value of 7.5 ± 1.0 μM and a maximum inhibition of 104 ± 6% were obtained with a Hill coefficient of 1.28 ± 0.09 ($n=12$) for cinnamophilin; corresponding values for diltiazem were $IC_{50}=1.5\pm0.5$ μM, maximal inhibition = 95 ± 4%, $n_H=1.14\pm0.09$ ($n=10$). Cinnamophilin accelerated the inactivation rate of $I_{Ca,L}$. The $I_{Ca,L}$ decay at 0 mV under control conditions ($n=12$) showed two time constants which are fast time constant (τ_f) = 36.9 ± 7.4 ms and slow time constant (τ_s) = 184.0 ± 30.8 ms. Comparative values in the presence of 3 μM cinnamophilin were $\tau_f=24.2\pm3.8$ ms and $\tau_s=144.8\pm27.8$ ms, and 10 μM cinnamophilin were $\tau_f=15.7\pm2.8$ ms ($P<0.05$) and $\tau_s=95.6\pm26.5$ ms, respectively. Figure 3d shows the *I–V* relationships of $I_{Ca,L}$ measured at the peak inward current. The averaged data indicate that cinnamophilin reduced peak current amplitude at any command voltage.

Effects of cinnamophilin on voltage-dependent activation, steady-state inactivation and recovery from inactivation of $I_{Ca,L}$

The steady-state activation curves of $I_{Ca,L}$ were derived from the *I–V* curves shown in Figure 3d. In Figure 3e, the normalized peak conductance of the Ca^{2+} channel was plotted as a function of membrane potential. The Boltzmann fitting yielded nearly identical values for either the half-maximal potential (V_h) or slope factor (k). On average ($n=10$), $V_h=-10.4\pm1.9$ mV and $k=5.4\pm0.4$ mV for control, and $V_h=-12.3\pm2.0$ mV and $k=5.4\pm0.3$ mV for 3 μM cinnamophilin, and $V_h=-12.8\pm2.0$ mV and $k=5.5\pm0.2$ mV for 10 μM cinnamophilin ($P>0.05$ for both V_h and k), respectively. Steady-state inactivation curves of $I_{Ca,L}$ were obtained by a double-pulse protocol shown in Figure 3e. The relationships between membrane potentials and the normalized current amplitude value evoked by the test pulse were fitted by the Boltzmann equation. Cinnamophilin (3 μM) shifted leftward the inactivation curve but did not significantly change the k value (Figure 3e). On average ($n=7$), $V_h=-27.0\pm1.2$ mV and $k=6.8\pm0.8$ mV for control, and $V_h=-54.9\pm3.1$ mV ($P<0.001$) and $k=8.3\pm0.5$ mV for 3 μM cinnamophilin, and $V_h=-64.7\pm3.4$ mV ($P<0.001$) and $k=6.1\pm0.6$ mV for 10 μM cinnamophilin, respectively.

The recovery of $I_{Ca,L}$ from inactivation was measured by use of a twin-pulse protocol as shown in the inset of Figure 3f. The fraction of recovery as a function of interpulse interval is shown in Figure 3f and can be well described by the sum of two exponentials. Cinnamophilin (1 and 3 μM) retarded the recovery of $I_{Ca,L}$ by reducing the proportion of the fast component of the recovering current from 0.68 ± 0.08 to 0.40 ± 0.09 ($P>0.05$, $n=7$) and 0.28 ± 0.08 ($P<0.05$, $n=7$), respectively. However, both the fast (τ_f) and slow (τ_s) recovery time constants were not significantly affected. On average ($n=7$), $\tau_f=0.22\pm0.05$ s and $\tau_s=3.82\pm0.88$ s for control, and $\tau_f=0.21\pm0.08$ s and $\tau_s=3.07\pm0.41$ s for 1 μM cinnamophilin, and $\tau_f=0.33\pm0.10$ s and $\tau_s=3.06\pm0.65$ s for 3 μM cinnamophilin, respectively.

Tonic and use-dependent effects of cinnamophilin on $I_{Ca,L}$

To determine whether cinnamophilin shows tonic and (or) use-dependent block on $I_{Ca,L}$, a train of 30 depolarizing pulses (300-ms in duration) to 0 mV at 0.5, 1 or 2 Hz was applied after a prepulse of –40 mV. Original sample traces of

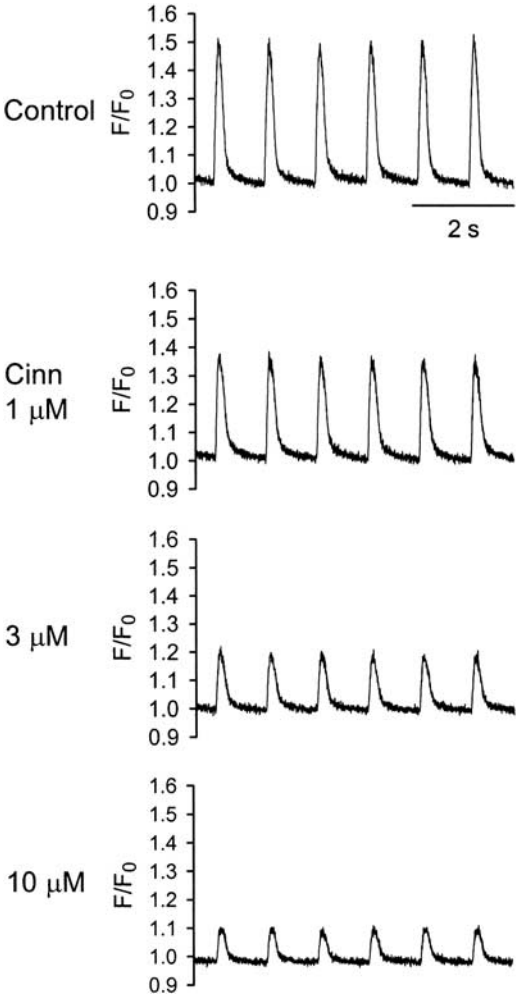

Figure 2 Concentration-dependent effects of cinnamophilin on intracellular Ca^{2+} transients in ventricular myocytes stimulated at 1 Hz. Original steady-state intracellular Ca^{2+} transients in the absence (control) and in the presence of 1, 3 and 10 μM cinnamophilin (Cinn) were measured using fluo-3 as relative fluorescence (F/F_0).

currents associated with the 1st, 2nd and 30th pulses are shown in Figure 4a. Under control conditions, peak $I_{Ca,L}$ amplitude hardly decreased after a train of 30 pulses at 0.5 and 1 Hz. The frequency dependence became more evident at 2 Hz (Figures 4a and b). The normalized peak $I_{Ca,L}$ amplitude of the 30th pulse at 0.5, 1 and 2 Hz were 98 ± 2, 100 ± 2 and 75 ± 2% ($n = 7$) to those of the first pulse, respectively. The magnitude of the tonic block of $I_{Ca,L}$ was measured as the percentage reduction of the normalized amplitude of $I_{Ca,L}$ elicited by the first pulse relative to the value before drug application. The tonic blocks of $I_{Ca,L}$ by 10 μM cinnamophilin were 34 ± 7, 40 ± 7 and 39 ± 6% (all $P < 0.01$, $n = 7$) at 0.5, 1 and 2 Hz, respectively (Figure 4b). Cinnamophilin produced a significant use-dependent inhibition on $I_{Ca,L}$. In the presence of 10 μM cinnamophilin, normalized peak $I_{Ca,L}$ amplitudes of the 30th pulse at 0.5, 1 and 2 Hz were 89 ± 6% ($P > 0.05$ vs control value as shown above), 66 ± 8% ($P < 0.01$), and 17 ± 3% ($P < 0.001$, $n = 7$) of the first pulse, respectively (Figure 4b). For comparison, the effects of diltiazem were also examined. The normalized peak $I_{Ca,L}$ amplitudes of the 30th pulse at 0.5, 1 and 2 Hz before diltiazem treatment were 100 ± 1, 100 ± 2 and 75 ± 4% ($n = 6$) of the first pulse, respectively. The tonic blocks of $I_{Ca,L}$ by 1 μM diltiazem were 46 ± 5, 52 ± 6 and 56 ± 6% (all $P < 0.001$, $n = 6$) at 0.5, 1 and 2 Hz, respectively. Diltiazem exerted significant use-dependent block on $I_{Ca,L}$ (figure not shown). In the presence of diltiazem, normalized peak $I_{Ca,L}$ amplitudes of the 30th pulse at 0.5, 1 and 2 Hz were 81 ± 7% ($P < 0.05$ vs control), 68 ± 6% ($P < 0.01$), and 22 ± 4% ($P < 0.001$, $n = 6$) of the first pulse, respectively.

Effects of cinnamophilin on I_{Na}

Figures 5a and b show typical superimposed current traces and *I–V* curves of I_{Na} elicited by step depolarizing pulses at 0.2 Hz, respectively. Cinnamophilin inhibited I_{Na} in a concentration-dependent manner. The concentration–response curve of the drug on I_{Na} at –20 mV (Figure 5c) yielded an IC_{50} of 2.7 ± 0.6 μM (maximum inhibition = 107 ± 6%, $n_H = 1.07 \pm 1.10$, $n = 9$). Figure 5d shows the voltage-dependent steady-state inactivation of I_{Na}. Cinnamophilin shifted the inactivation curve to the left but did not alter the *k* value. On average ($n = 7$), $V_h = -66.6 \pm 2.6$ mV and $k = 4.7 \pm 0.3$ mV for control, and $V_h = -76.1 \pm 2.9$ mV and $k = 5.4 \pm 0.2$ mV for 3 μM cinnamophilin, and $V_h = -83.6 \pm 3.4$ mV ($P < 0.05$) and $k = 5.6 \pm 0.3$ mV for 10 μM cinnamophilin, respectively. Figure 5e shows the recovery of I_{Na} from inactivation in the control conditions could be well fitted by a two exponential function. In the presence of cinnamophilin, the proportion of fast recovery component (*A*) was reduced and the time course (τ_f) of this component was prolonged markedly. On average ($n = 7$), $A = 0.76 \pm 0.06$, $\tau_f = 36.5 \pm 14.4$ ms, and $\tau_s = 176.7 \pm 19.2$ ms for control, and $A = 0.62 \pm 0.08$, $\tau_f = 84.8 \pm 18.5$ ms, and $\tau_s = 280.5 \pm 61.5$ ms for 3 μM cinnamophilin, and $A = 0.47 \pm 0.08$ ($P < 0.05$), $\tau_f = 135.1 \pm 22.5$ ms ($P < 0.01$), and $\tau_s = 319.2 \pm 69.6$ ms for 10 μM cinnamophilin, respectively.

Effects of cinnamophilin on K^+ currents

I_K was elicited by a family of 3-s depolarizing pulses (–20 to + 60 mV) from a holding potential of –40 mV. Cinnamophilin (10 μM) slightly decreased the time-dependent I_K during the depolarizing pulse and the $I_{K,tail}$ appearing on return to –40 mV (Figure 6a). Figure 6b shows the *I–V* relationships for $I_{K,tail}$ currents. At the potential of + 60 mV, 1, 3 and 10 μM cinnamophilin reduced $I_{K,tail}$ density from the control value of 1.20 ± 0.26 pA pF^{-1} to 1.01 ± 0.19, 0.87 ± 0.19 and 0.65 ± 0.12 pA pF^{-1} ($n = 9$, all $P > 0.05$), respectively.

I_{K1} was elicited by step protocols from –120 to 0 mV in 10 mV increments after a prepulse of –40 mV. Figures 6c and d show sample traces and *I–V* curves of I_{K1}, respectively. Cinnamophilin induced a slight but insignificant decrease in both the inward and outward I_{K1} amplitudes. Cinnamophilin at 3 and 10 μM reduced I_{K1} density at –30 mV from the control value of 4.7 ± 1.0 pA pF^{-1} to 3.4 ± 0.8 and 2.2 ± 0.4 pA pF^{-1} ($n = 8$), respectively, and reduced this current at –120 mV from –18.8 ± 3.7 pA pF^{-1} to –16.9 ± 3.1 and –14.4 ± 2.5 pA pF^{-1} ($n = 8$), respectively.

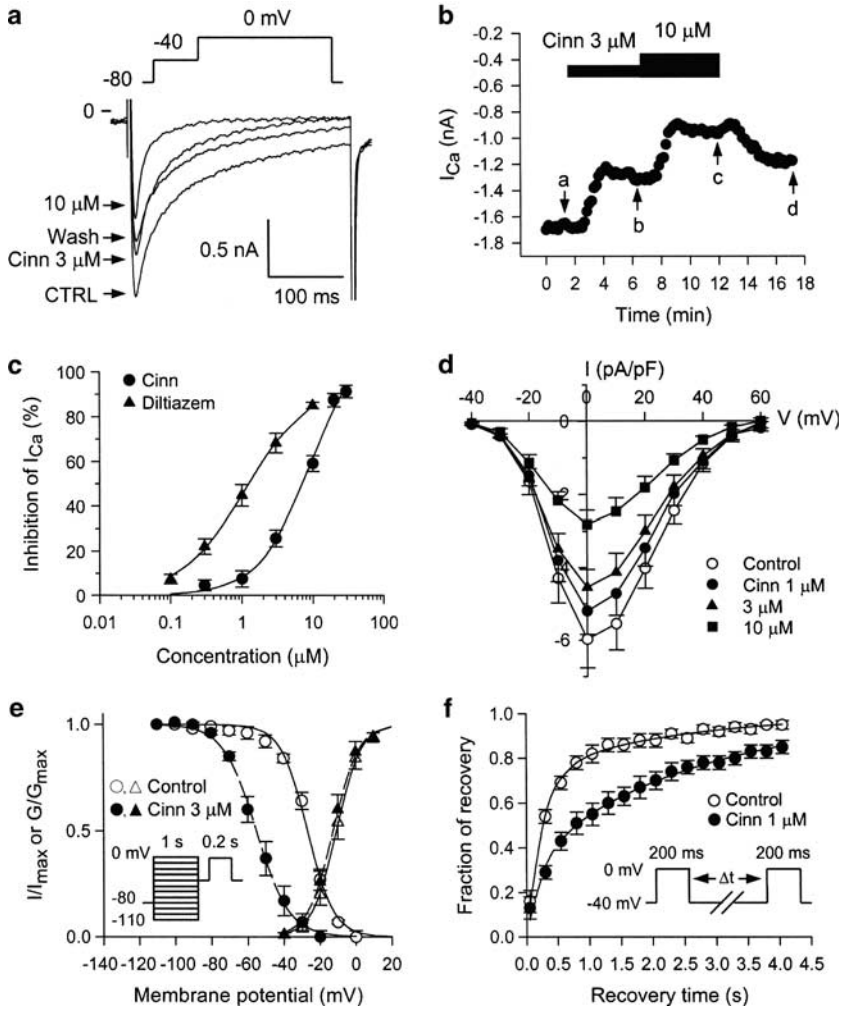

Figure 3 Effects of cinnamophilin on $I_{Ca,L}$ recorded in guinea-pig ventricular myocytes. (**a**) Individual sample traces recorded in one myocyte in response to 300 ms steps to 0 mV in the absence, in the presence of 3 and 10 μM cinnamophilin (Cinn), and after washout of drug. Each step to 0 mV was preceded by a 150-ms prestep to –40 mV (holding potential = −80 mV; pulse protocol shown at top). (**b**) Time courses of alteration of $I_{Ca,L}$ amplitude. Step pulses were applied every 10 s. Letters on the curve correspond to traces in (**a**) (point a: control; point b: Cinn 3 μM; point c: Cinn 10 μM and point d: washout). (**c**) Concentration–response curves for the effect of cinnamophilin ($n = 12$) and diltiazem ($n = 10$) on $I_{Ca,L}$. Solid lines were drawn by fitting to the Hill equation. (**d**) *I–V* curves of $I_{Ca,L}$ in the absence (control) and presence of different concentrations of cinnamophilin. Each data point represents means ± s.e.mean from 10 cells. $I_{Ca,L}$ was elicited by various depolarizing pulses (300 ms duration) ranging from −40 to + 60 mV in 10 mV increments at 0.1 Hz. (**e**) Voltage dependence of steady-state $I_{Ca,L}$ activation and inactivation in the absence and presence of 3 μM cinnamophilin. The activation curves were constructed using *I–V* relationships shown in (**d**). Normalized Ca^{2+} conductance is plotted as a function of the membrane potential ($n = 10$). Smooth curves are Boltzmann fittings for control (solid line) and cinnamophilin-treated (dashed line) groups. Voltage-dependent steady-state inactivation was examined with a two-pulse protocol as shown in the inset. Preconditioning pulses of 1 s duration were applied in 10 mV steps between −110 and 0 mV from a holding potential of −80 mV, and then the test pulse of 200 ms duration was applied to 0 mV (interpulse duration was 30 ms). The inactivation curves were obtained by normalizing the current amplitudes (*I*) to the maximal value (I_{max}) and plotted as a function of the prepulse potential in the absence and presence of 3 μM cinnamophilin ($n = 7$). (**f**) Effects of cinnamophilin on the recovery of $I_{Ca,L}$ from inactivation. Recovery was measured by a double-pulse protocol (see inset). Both pre- and test-pulse were stepped to 0 mV with identical duration of 200 ms and the pulse interval was varied between 50 and 4050 ms. Each two-pulse sequence was separated by a 30 s interval. The ratio of $I_{Ca,L}$ obtained by the test pulse to that elicited by the prepulse (fraction of recovery) is plotted as a function of the interpulse interval. Solid and dashed lines represent biexponential curves fitted to the data in control and cinnamophilin-treated groups ($n = 7$), respectively. $I_{Ca,L}$, L-type Ca^{2+} inward current; *I–V*, current–voltage.

Typical whole-cell current recordings evoked by voltage-ramps from ventricular myocytes are shown in Figures 6e and f. These figures demonstrate a pronounced increase in $I_{K,ATP}$ both in the outward and inward direction after application of 100 μM cromakalim. Cinnamophilin produced a concentration-dependent inhibition of the cromakalim-evoked currents (Figure 6e). At the potential of 0 mV, 1, 3, 10 and 30 μM cinnamophilin reduced $I_{K,ATP}$ by 24 ± 6, 35 ± 9, 50 ± 9 and 79 ± 10% ($n = 7$), respectively. Glibenclamide, a typical ATP-sensitive K^+ channel (K_{ATP}) blocker, also inhibited the current potently (Figure 6f). $I_{K,ATP}$ was reduced by 11 ± 4, 33 ± 10, 62 ± 10 and 76 ± 10% ($n = 7$) after 1, 3, 10 and 30 nM glibenclamide, respectively.

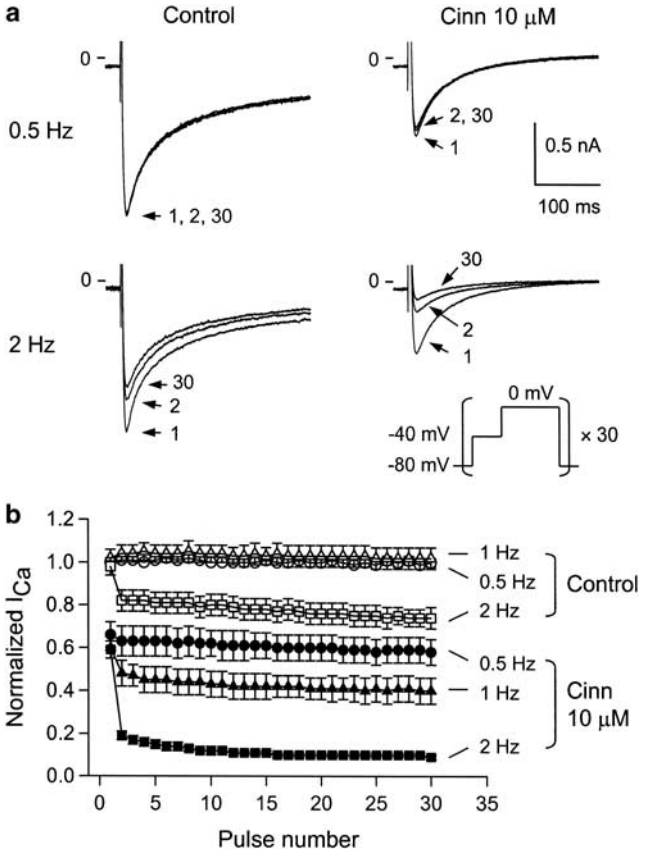

Figure 4 Tonic block and use-dependent block of $I_{Ca,L}$. (**a**) Original recordings of $I_{Ca,L}$ obtained under control conditions and in the presence of cinnamophilin (10 μM). $I_{Ca,L}$ were elicited by 30 consecutive 300 ms depolarizing step pulses to 0 mV (each one preceded by a 150-ms prepulse to −40 mV from a holding potential of −80 mV) at 0.5 Hz (upper) or 2 Hz (lower). The pulse protocol is shown in the inset. For each condition, pulses 1, 2 and 30 are shown. (**b**) Peak amplitudes of $I_{Ca,L}$ were normalized to that elicited by the first test pulse before drug application at 0.5 Hz and plotted against the number of pulses applied at different rates in the absence and presence of cinnamophilin (10 μM). Each data point represents means ± s.e.mean ($n=7$). $I_{Ca,L}$, L-type Ca^{2+} inward current.

Modification of the electrophysiological properties of the cardiac conduction system

An example of intracardiac electrograms after cinnamophilin treatment is shown in Figure 7 and the averaged data are summarized in Table 2. Cinnamophilin (⩾3 μM) caused a concentration-dependent prolongation in the AV nodal refractory period and WCL. At higher concentrations (⩾30 μM), the AH interval and the VERP were also prolonged, while the VRT was shortened by this agent. The conduction interval through the atrial tissue (SA) and His-Purkinje system (HV), the BCL and the refractory period of atrium were not significantly changed. In the present experimental protocol, the AV node usually became refractory to premature extrastimulation before the His-Purkinje system became refractory. Therefore, only the functional refractory period of the His-Purkinje system (shortest conducted V_1V_2 interval) was measured. This parameter was significantly prolonged by higher concentrations (⩾30 μM) of cinnamophilin.

Anti-arrhythmic effect in isolated hearts

Arrhythmias induced by reperfusion appeared within 10–30 s. In either DMSO or saline vehicle control groups, the ventricular fibrillation (VF) incidence was 100% and lasted for about 4–5 min then returned spontaneously to normal sinus rhythm thereafter. Typical electrograms recorded from a DMSO- and a cinnamophilin (30 μM)-perfused heart are shown in Figures 8a and b, respectively. Cinnamophilin (10 and 30 μM) and diltiazem (3 μM) significantly reduced both incidence and duration of VF compared with those of the DMSO-perfused group (Table 3). However, these parameters in the group treated with the TXA_2 receptor antagonist SQ29548 (1 μM) plus the TXA_2 synthase inhibitor ozagrel (30 μM) and in that treated with glibenclamide (1 μM) were not different from those in the DMSO group. Similarly, these parameters in hearts treated with the free-radical scavengers, superoxide dismutase (SOD) (100 U ml^{-1}) plus catalase (500 U ml^{-1}), were identical to those of the saline group.

Discussion

The present study significantly expands on the study of Su *et al*. (1999) and contributes new insights into the mechanisms of action of cinnamophilin. The novel findings of this study are that the effects of cinnamophilin on the conduction functions and electromechanical properties in guinea-pig cardiac preparations are mainly due to the inhibition of Ca^{2+} and Na^+ inward currents, although the K^+-repolarizing currents were also inhibited somewhat. Similarly, the anti-arrhythmic effect of cinnamophilin is likely to be related to its ability to block Ca^{2+} and Na^+ channels.

The cardiac APD is maintained by a delicate balance between inward and outward ionic currents flowing at a similar time course in opposite directions. Three major K^+ currents, I_K, I_{to} and I_{K1}, mediate different phase of the repolarization process (Nerbonne and Kass, 2005). I_{to} is the predominant repolarizing current in rat ventricular myocytes (Josephson *et al*., 1984). While in guinea-pig ventricular tissues, little I_{to} is available for repolarization and the dominant outward currents are the I_K and I_{K1} (Hume and Uehara, 1985). A previous report documented that cinnamophilin caused a prolongation of APD in rat ventricular myocytes (Su *et al*., 1999), whereas the present study conducted in guinea-pig papillary muscles showed a contrary result. The interspecies differences in the modulation of APD by cinnamophilin can be explained by the shorter APD in rat ventricle which would be more sensitive to I_{to} blockade ($IC_{50}=7.1$ μM) and subsequent delay of repolarization in spite of the concomitant blockade of $I_{Ca,L}$ ($IC_{50}=9.5$ μM) and I_{Na} ($IC_{50}=10$ μM) (Su *et al*., 1999). However, the longer plateau duration of action potentials in guinea-pig ventricle may augment the shortening influence related to inhibition of $I_{Ca,L}$ and I_{Na}, which could outweigh the minor lengthening effect due to the lesser blockade of the outward K^+ currents, by cinnamophilin.

Our voltage–clamp study demonstrated that cinnamophilin blocked cardiac Na^+ channels and such actions may contribute to its suppression of V_{max} of action potential in papillary muscle and the prolongation of His-Purkinje

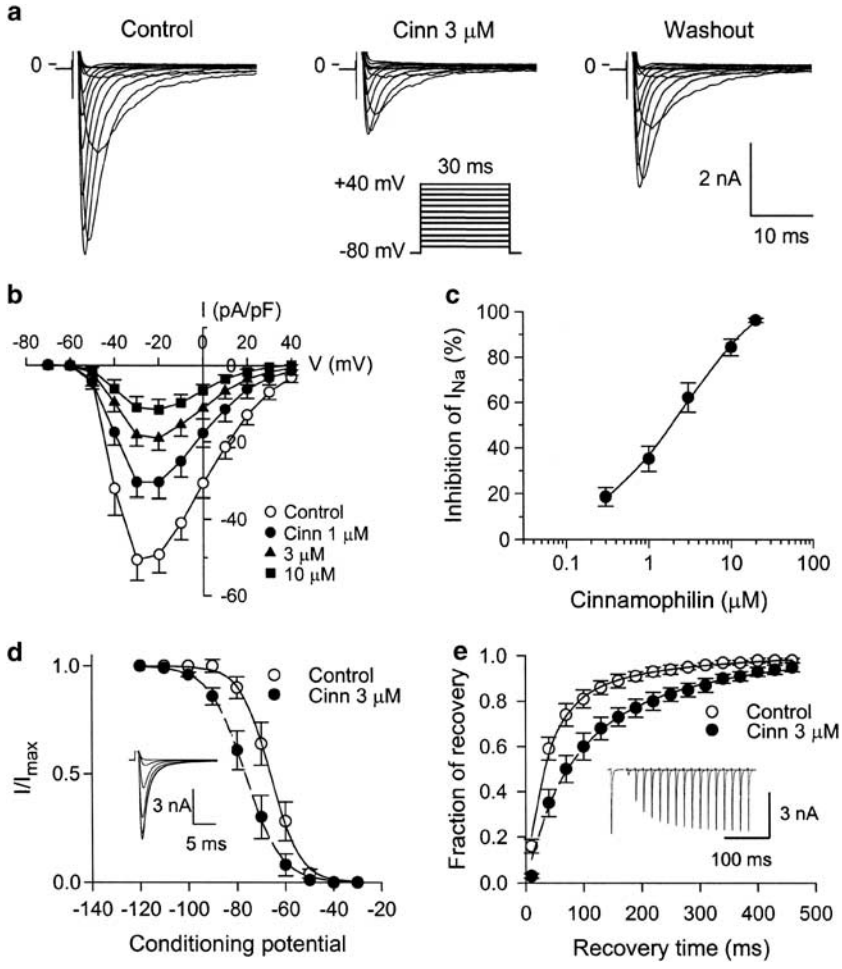

Figure 5 Effects of cinnamophilin on I_{Na} in guinea-pig ventricular myocytes. (**a**) Superimposed current traces elicited by 30 ms depolarizing test pulses (–70 to +40 mV in 10 mV increments) from a holding potential of –80 mV, before (control), 5 min after bath application of 3 μM cinnamophilin, and upon 5-min washout. The pulse protocol is shown in the inset. (**b**) *I–V* curves of I_{Na} in the absence and presence of 1, 3 and 10 μM cinnamophilin. Data are means ± s.e.mean ($n=7$). (**c**) Concentration–response curve for cinnamophilin on I_{Na} is shown. Solid curve was drawn by fitting to the Hill equation. I_{Na} was elicited by a series of 30 ms test pulses to –20 mV from a holding potential of –80 mV at 0.2 Hz. (**d**) Voltage dependence of steady-state I_{Na} inactivation in the absence and presence of 3 μM cinnamophilin. Conditioning pulses (1 s long) to potentials ranging from –120 to –30 mV were applied before 50 ms depolarizing test pulses to –20 mV. The holding potential was –80 mV. The predrug superimposed current traces are shown in the inset. Solid and dashed lines drawn through the data points were the best fit to the Boltzmann equation before and after cinnamophilin ($n=7$), respectively. (**e**) Recovery of I_{Na} from inactivation in the absence and presence of 3 μM cinnamophilin. The twin-pulse protocol used consisted of a 50 ms prepulse from –80 to –20 mV was followed after various recovery times by a 20 ms test pulse to –20 mV. An example of control current traces is shown in the inset. The normalized current is plotted against the recovery time. Lines (control, solid line; cinnamophilin, dashed line) show best-fits of a double exponential function to the data ($n=7$). I_{Na}, Na^+ inward current; *I–V*, current–voltage.

system functional refractory period in isolated heart. The inhibitory effect of cinnamophilin on Na^+ channels was characterized by a leftward shift of the voltage-dependent inactivation curve and a retardation of recovery from inactivation of this channel. It has been proposed that the affinity of Na^+ channel blockers for the inactivated and resting state channels could be estimated by the following equation (Bean *et al*., 1983): $\Delta V_h = k \times \ln[(1 + C/K_r)/(1 + C/K_i)]$, where the ΔV_h is the shift in the midpoint, k is the slope factor, C is the concentration of compound, and K_r and K_i are the dissociation constants for rested and inactivated channels, respectively. From the ΔV_h obtained at 3 and 10 μM of cinnamophilin, the values of K_i and K_r were calculated to be 0.6 and 285.7 μM, respectively. These results suggest that cinnamophilin may bind preferentially to the inactivated channel, resulting in a decrease of the available channels for activation. Another interesting finding of this study is that cinnamophilin prolonged VERP but shortened both the APD and VRT in isolated heart. This may be ascribed to the drug-induced delay of recovery of Na^+ channel from the inactivated state and subsequent extension of the post-repolarization refractoriness. The disparity between the concentrations of cinnamophilin required to prolong VERP and those binding to inactivated Na^+ channels may be due to the differences in experimental conditions. Recordings of I_{Na} were obtained from single myocytes in low Na^+ solutions and such lower I_{Na} amplitude would enhance the effect of the drug. However, experiments on VERP were performed in isolated heart perfused with normal Tyrode solution, in which conditions of the Na^+ gradient is normal and the

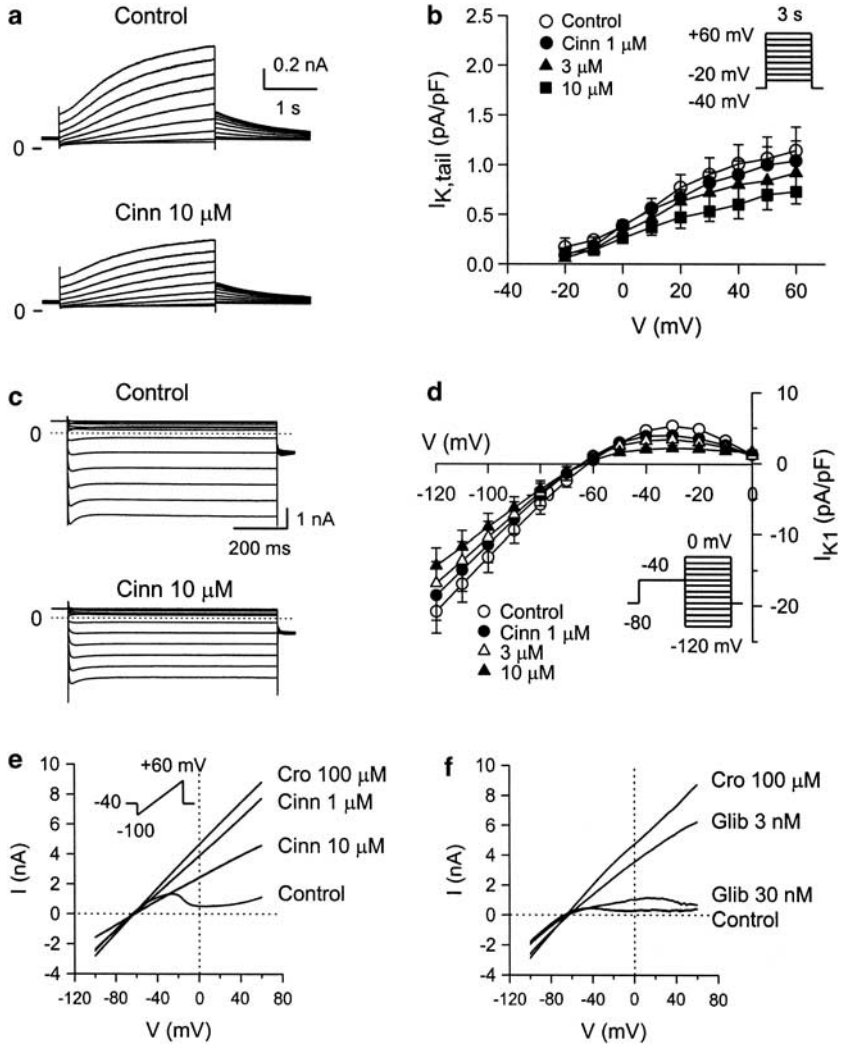

Figure 6 (**a**) Effects of cinnamophilin on I_K in guinea-pig ventricular myocytes. Superimposed current traces obtained during 3 s depolarizing pulses to potentials ranging from −20 to +60 mV in 10 mV steps applied from a holding potential of –40 mV before (control) and after 5 min exposure to 10 μM cinnamophilin. (**b**) *I–V* relationships for I_K tail currents recorded under control conditions and during exposure to increasing concentrations of cinnamophilin. Data are means ± s.e.mean ($n=9$). (**c**) Effects of cinnamophilin on I_{K1} in ventricular myocytes. Superimposed current traces in the absence and after 5 min of exposure to 10 μM cinnamophilin were serially elicited (from 0 to –120 mV for 800 ms in 10 mV steps) after a prepulse of –40 mV. (**d**) *I–V* curves of I_{K1} in the absence and presence of 1, 3, and 10 μM cinnamophilin. Data are means ± s.e.mean ($n=8$). (**e**) and (**f**) Effects of cinnamophilin (Cinn) or glibenclamide (Glib) on whole-cell $I_{K,ATP}$ induced by 100 μM cromakalim (Cro) in ventricular myocytes, respectively. The quasi steady-state currents were evoked by a 9-s long voltage ramp from −100 to +60 mV (holding potential = –40 mV). The voltage protocol is shown in the inset of (**e**). I_K, delayed rectifier K^+ current; I_{K1}, inward rectifier K^+ current; $I_{K,ATP}$, ATP-sensitive K^+ current; *I–V*, current–voltage.

access of drug to its target site is not as easy as that in single cell studies.

Also, our results showed that cinnamophilin inhibited $I_{Ca,L}$ in guinea-pig ventricular myocytes, similar its effect in rat cardiomyocytes (Su *et al*., 1999). Cinnamophilin exerted a use-dependent block of $I_{Ca,L}$, as observed with the classic Ca^{2+} antagonists such as verapamil and diltiazem (Lee and Tsien, 1983; Hering *et al*., 1998), indicating that these agents preferentially bind Ca^{2+} channels that are in the open or inactivated state (or both). The finding that cinnamophilin caused a negative shift of the inactivation curve and a delay of recovery from inactivation of Ca^{2+} channel suggests that this agent can interact with inactivated channels with a slow dissociation rate. These results may also partly explain the tonic block caused by cinnamophilin, although the underlying mechanisms may also include blockade of channels in the resting state. Cinnamophilin accelerated the decay of $I_{Ca,L}$ suggests that it may also act through blocking the open channels. In the isolated heart study, cinnamophilin displayed marked frequency-dependent depression of AV nodal conduction as manifested by the prolongation of the AV nodal conduction interval, refractory period and WCL. This effect may be explained through its direct suppression of $I_{Ca,L}$. In addition, the negative inotropic effect of cinnamophilin could also be explained by Ca^{2+} channel antagonism and subsequent decrease in the Ca^{2+} transient (Grantham and Cannel, 1996).

Reperfusion following myocardial ischaemia often causes severe ventricular arrhythmias such as ventricular tachycardia and fibrillation. The mechanism(s) underlying the

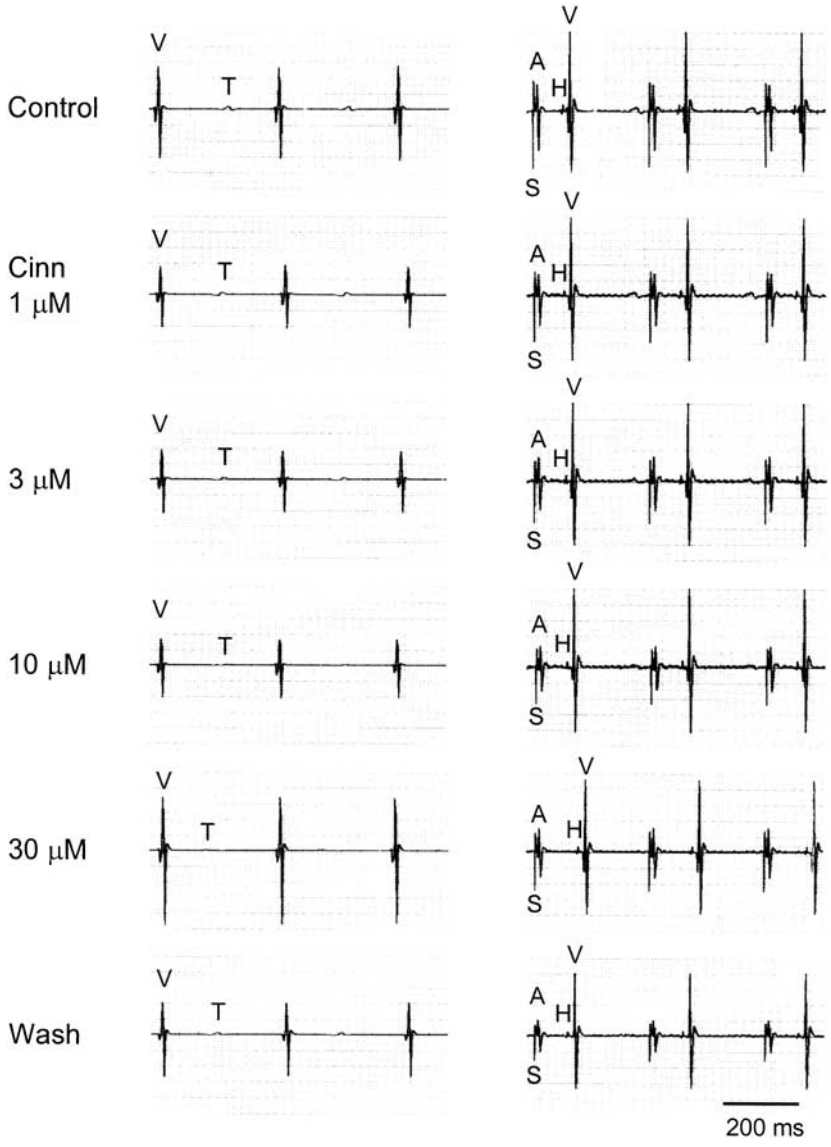

Figure 7 Representative ventricular electrograms at spontaneous rhythm (left) and His bundle electrograms at paced rhythm (300 ms cycle length, right) after cinnamophilin (Cinn) of the guinea-pig heart. A, atrial depolarization; H, His bundle depolarization; S, stimulation artifact; T, ventricular repolarization; V, ventricular depolarization. The paper speed was 100 mm s^{-1}.

Table 2 Concentration-related effects of cinnamophilin on the conduction system of guinea-pig isolated heart

	Cinnamophilin (μM)					
	Control	*1*	*3*	*10*	*30*	*Washout*
BCL	309 ± 8	315 ± 8	316 ± 8	317 ± 8	321 ± 7	310 ± 6
SA	12 ± 1	12 ± 1	13 ± 1	13 ± 1	14 ± 2	13 ± 1
AH	56 ± 2	58 ± 2	59 ± 2	62 ± 3	72 ± 3*	66 ± 3
HV	16 ± 1	15 ± 1	16 ± 1	17 ± 2	17 ± 1	16 ± 1
VRT	181 ± 4	176 ± 4	170 ± 6	168 ± 6	159 ± 8*	169 ± 5
WCL	183 ± 4	193 ± 5	204 ± 5*	214 ± 6**	234 ± 7***	203 ± 6
AERP	62 ± 3	67 ± 4	68 ± 4	72 ± 3	77 ± 4	69 ± 6
AVNERP	143 ± 4	159 ± 6	171 ± 7*	186 ± 7***	215 ± 8***	179 ± 8*
HPFRP	227 ± 5	229 ± 5	242 ± 6	247 ± 6	256 ± 7*	246 ± 8
VERP	154 ± 5	152 ± 6	153 ± 7	166 ± 5	182 ± 7*	150 ± 6

Abbreviations: AH, atrio-His bundle conduction interval; AERP, atrial effective refractory period; AVNERP, AV nodal effective refractory period; BCL, basic cycle length; HPFRP, His-Purkinje system functional refractory period; HV, His-ventricular conduction interval; SA, sinoatrial conduction interval; VERP, ventricular effective refractory period; VRT, ventricular repolarization time (VT interval); WCL, Wenckebach cycle length.
Data (in ms) were obtained from 14 experiments and are expressed as means ± s.e.mean.
*$P<0.05$, **$P<0.01$ and ***$P<0.001$ compared to respective control value by ANOVA, followed by Dunnett's *t*-test for multiple comparisons.

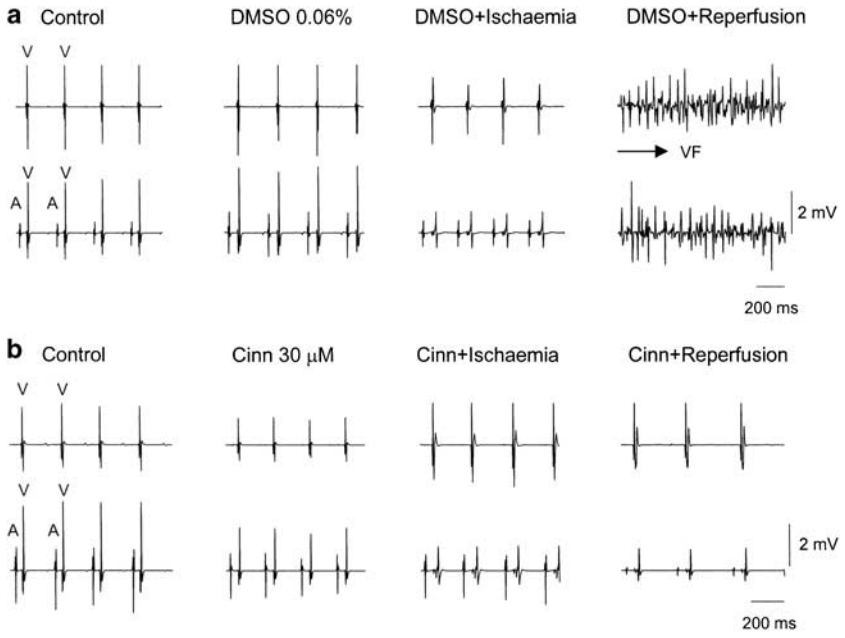

Figure 8 Protection against globally ischaemia/reperfusion-induced arrhythmias by cinnamophilin. (**a**) Electrogram recorded from a DMSO-perfused control heart in which VF can be readily induced after ischaemia/reperfusion. (**b**) Electrogram recorded from a cinnamophilin (30 μM)-perfused heart which maintained sinus rhythm after ischaemia/reperfusion. Upper and lower traces in both (**a**) and (**b**) show the ventricular electrogram and the electrogram recorded at lower atrium, respectively, and show the atrial (A) and ventricular depolarization (V). DMSO, dimethylsulphoxide; VF, ventricular fibrillation.

Table 3 Effects of cinnamophilin, diltiazem, SQ29548 with ozagrel, glibenclamide and SOD with catalase, on reperfusion-induced VF in guinea-pig isolated hearts

Groups	*n*	*Incidence of VF*	*Duration of VF (s)*
DMSO control 0.06%	10	10/10 (100%)	282 ± 21
Cinnamophilin 10 μM	10	5/10 (50%)*	13 ± 5***
30 μM	9	3/9 (33%)**	5 ± 2***
Diltiazem 3 μM	10	4/10 (40%)*	56 ± 30***
SQ29548 1 μM + ozagrel 30 μM	8	8/8 (100%)	288 ± 42
Glibenclamide 1 μM	11	11/11 (100%)	258 ± 51
Saline control 0.025 ml ml^{-1}	12	12/12 (100%)	268 ± 65
SOD 100 U ml^{-1} + catalase 500 U ml^{-1}	10	10/10 (100%)	275 ± 47

Abbreviations: DMSO, dimethylsulphoxide; SOD, superoxide dismutase; VF, ventricular fibrillation.
Values of duration of VF are expressed as mean ± s.e.mean. Different concentrations of drug stock solutions were used to obtain an equivalent DMSO vehicle concentration of 0.06%.
*$P<0.05$ and **$P<0.01$ compared with DMSO vehicle control value by Fisher's exact test; ***$P<0.001$ compared with DMSO vehicle control group by ANOVA, followed by Dunnett's *t*-test for multiple comparisons.

genesis of such lethal arrhythmias are complex but may include the formation of oxygen-derived free radicals, the heterogeneity of damage and recovery in cardiomyocytes and excess cytosolic Ca^{2+} loading (Manning and Hearse, 1984; Pogwizd and Corr, 1987; Opie *et al*., 1988). These might lead to electrophysiological disturbances including the re-entry process and enhanced automaticity such as oscillatory afterpotentials (Manning and Hearse, 1984). Both Ca^{2+} and Na^{+} channel blockers are reported effectively to suppress reperfusion arrhythmias (Opie *et al*., 1988; Tosaki *et al*., 1988; Swies *et al*., 1990; Wang *et al*., 2002). It is possible that the anti-arrhythmic ability of cinnamophilin may arise mainly from the inhibition of $I_{Ca,L}$ and I_{Na}, which, in turn, would decrease the intracellular free Ca^{2+} concentration and thereby may contribute to the suppression of oscillatory afterpotentials produced by Ca^{2+} overload. More importantly, the high affinity of cinnamophilin for inactivated channels may cause this agent to act preferentially on partially depolarized tissues in pathological conditions. Consequently, the reduction of Ca^{2+} influx under such conditions may contribute to a decrease in the formation of re-entry circuits (Kléber, 1992). In addition, the prolongation of VERP through inhibition of I_{Na} may also play a part in the attenuation of the re-entry-induced VF.

Other mechanisms whereby cinnamophilin could have a beneficial effect against reperfusion arrhythmias were also considered in our study. The failure of free-radical scavengers (SOD with catalase) to prevent reperfusion-induced VF implies that the anti-arrhythmic action of cinnamophilin might not be attributable to its antioxidant effect in the present model. It has also been shown that TXA_2, a vasoconstrictor as well as a promoter of platelet aggregation that is abnormally released during ischaemia, is arrhythmogenic and important in the development of VF after reperfusion (Coker *et al*., 1981; Coker, 1984). Consequently, several studies reported that TXA_2 synthase inhibitors or TXA_2 receptor antagonists could reduce or prevent ischaemia-induced arrhythmias in anaesthetized animals (Coker, 1984; Ogura *et al*., 1988). However, the dual TXA_2 synthase and receptor inhibitory activities of cinnamophilin were not likely to be related to its anti-arrhythmic action here, as the combination of ozagrel and SQ29548 was ineffective in the

present *in vitro* model. During myocardial ischaemia, the activation of K_{ATP} promotes K^+ efflux, reduction in APD, and inhomogeneities in repolarization creating a substrate for re-entry (Billman, 1994). It is thus conceivable that K_{ATP} blockers such as glibenclamide could play a role in the prevention of ventricular arrhythmias during ischaemia (El-Reyani *et al*., 1999; Dhein *et al*., 2000). However, negative or contrary reports have also been presented (Cole *et al*., 1991; Bernauer, 1997), including the result of this study. In fact, opening of the K_{ATP} also has been implicated as a cardioprotective mechanism underlying ischaemia-related preconditioning (Grover, 1994). The results from our study imply that the moderate inhibition of K_{ATP} by cinnamophilin does not contribute to its anti-arrhythmic action in the present model.

In conclusion, our results clearly indicate that cinnamophilin, a natural compound with multiple pharmacological actions, is effective in preventing reperfusion-induced ventricular arrhythmias in guinea-pig hearts. The anti-arrhythmic effect and the modification of the electromechanical functions by cinnamophilin are likely to result mainly from its blockade of $I_{Ca,L}$ and I_{Na}, that is, class IV and class I anti-arrhythmic actions. The inhibition of I_{Ca} by cinnamophilin is similar to that by diltiazem. Although the unique TXA_2 antagonistic and anti-oxidative actions of cinnamophilin seem not to be involved in its anti-arrhythmic actions in the present model, it remains possible that they would provide some additional benefits *in vivo*, where the levels of TXA_2 or oxidative stress are elevated above normal.

Acknowledgements

We thank Ms Miao-Sui Lin, Ms Ya-Chin Wang and Mr Chih-Wei Hsieh for their technical assistance. The present work was supported by grants from the Chang Gung Medical Research Foundation (CMRP1231) and National Science Council (NSC90-2315-B-182-004) of Taiwan.

Conflict of interest

The authors state no conflict of interest.

References

Bean BP, Cohen AJ, Tsien RW (1983). Lidocaine block of cardiac sodium channels. *J Gen Physiol* **81**: 613–642.

Bernauer W (1997). Concerning the effect of the K^+ channel blocking agent glibenclamide on ischaemic and reperfusion arrhythmias. *Eur J Pharmacol* **326**: 147–156.

Billman GE (1994). Role of ATP sensitive potassium channel in extracellular potassium accumulation and cardiac arrhythmias during myocardial ischaemia. *Cardiovasc Res* **28**: 762–769.

Chang GJ, Su MJ, Hung LM, Lee SS (2002). Cardiac electrophysiologic and antiarrhythmic actions of a pavine alkaloid derivative, *O*-methyl-neocaryachine, in rat heart. *Br J Pharmacol* **136**: 459–471.

Chang GJ, Su MJ, Kuo SC, Lin TP, Lee YS (2006). Multiple cellular electrophysiological effects of a novel antiarrhythmic furoquinoline derivative HA-7 [*N*-benzyl-7-methoxy-2,3,4,9-tetrahydrofuro[2,3-*b*]quinoline-3,4-dione] in guinea pig cardiac preparations. *J Pharmacol Exp Ther* **316**: 380–391.

Cheng HT, Chang H (1995). Reduction of reperfusion injury in rat skeletal muscle following administration of cinnamophilin, a novel dual inhibitor of thromboxane synthase and thromboxane A_2 receptor. *Thorac Cardiovasc Surg* **43**: 73–76.

Coker SJ (1984). Further evidence that thromboxane exacerbates arrhythmias: effects of UK38485 during coronary artery occlusion and reperfusion in anaesthetized greyhounds. *J Mol Cell Cardiol* **16**: 633–641.

Coker SJ, Parratt JR, Ledingham IM, Zeitlin IJ (1981). Thromboxane and prostacyclin release from ischaemic myocardium in relation to arrhythmias. *Nature* **291**: 323–324.

Cole WC, McPherson CD, Sontag D (1991). ATP-regulated K^+ channels protect the myocardium against ischemia/reperfusion damage. *Circ Res* **69**: 571–581.

Dhein S, Pejman P, Krusemann K (2000). Effects of the $I_{(K.ATP)}$ blockers glibenclamide and HMR1883 on cardiac electrophysiology during ischemia and reperfusion. *Eur J Pharmacol* **398**: 273–284.

El-Reyani NE, Bozdogan O, Baczko I, Lepran I, Papp JG (1999). Comparison of the efficacy of glibenclamide and glimepiride in reperfusion-induced arrhythmias in rats. *Eur J Pharmacol* **365**: 187–192.

Grantham CJ, Cannel MB (1996). Ca^{2+} influx during the cardiac action potential in guinea pig ventricular myocytes. *Circ Res* **79**: 194–200.

Grover GJ (1994). Protective effects of ATP-sensitive potassium-channel openers in experimental myocardial ischemia. *J Cardiovasc Pharmacol* **24** (Suppl 4): S18–S27.

Hering S, Berjukow S, Aczél S, Timin EN (1998). Ca^{2+} channel block and inactivation: common molecular determinants. *Trends Pharmacol Sci* **19**: 439–443.

Hsiao G, Teng CM, Sheu JR, Cheng YW, Lam KK, Lee YM *et al*. (2001). Cinnamophilin as a novel antioxidative cytoprotectant and free radical scavenger. *Biochim Biophys Acta* **1525**: 77–88.

Hume JR, Uehara A (1985). Ionic basis of the different action potential configurations of single guinea-pig atrial and ventricular myocytes. *J Physiol (London)* **368**: 525–544.

Josephson IR, Sanchez-Chapula J, Brown AM (1984). Early outward current in rat single ventricular cells. *Circ Res* **54**: 157–162.

Kléber G (1992). The potential role of Ca^{2+} for electrical cell-to-cell uncoupling and conduction block in myocardial tissue. *Basic Res Cardiol* **87** (Suppl 2): 131–143.

Lee KS, Tsien RW (1983). Mechanism of calcium channel blockade by verapamil, D600, diltiazem and nitrendipine in single dialysed heart cells. *Nature* **302**: 193–209.

Li GR, Feng J, Yue L, Carrier M, Nattel S (1996). Evidence for two components of delayed rectifier K^+ current in human ventricular myocytes. *Circ Res* **78**: 689–696.

Manning AS, Hearse DJ (1984). Reperfusion-induced arrhythmias: mechanism and prevention. *J Mol Cell Cardiol* **16**: 497–518.

Nerbonne JM, Kass RS (2005). Molecular physiology of cardiac repolarization. *Physiol Rev* **85**: 1205–1253.

Ogura T, Watanabe I, Saito T, Saito S, Ozawa Y, Hatano M (1988). Effects of OKY-046, a selective thromboxane A_2 synthetase inhibitor, on ventricular arrhythmias and prostaglandins during coronary artery ligation and reperfusion in anesthetized dogs. *Jpn J Pharmacol* **47**: 95–98.

Opie LH, Coetzee WA, Dennis SC, Thandroyen FT (1988). A potential role for calcium ions in early ischemic and reperfusion arrhythmias. *Ann N Y Acad Sci* **522**: 464–477.

Pogwizd SM, Corr PB (1987). Electrophysiologic mechanisms underlying arrhythmias due to reperfusion of ischemic myocardium. *Circulation* **76**: 404–426.

Su MJ, Chen WP, Lo TY, Wu TS (1999). Ionic mechanisms for the antiarrhythmic action of cinnamophilin in rat heart. *J Biomed Sci* **6**: 376–386.

Swies J, Omogbai KI, Smith GM (1990). Occlusion and reperfusion-induced arrhythmias in rats: involvement of platelets and effects of calcium antagonists. *J Cardiovasc Pharmacol* **15**: 816–825.

Tosaki A, Balint S, Szekeres L (1988). Protective effect of lidocaine against ischemia and reperfusion-induced arrhythmias and shifts

of myocardial sodium, potassium and calcium content. *J Cardiovasc Pharmacol* **12**: 621–628.

Varró A, Lathrop DA, Hester SB, Nanasi PP, Papp JG (1993). Ionic currents and action potentials in rabbit, rat, and guinea pig ventricular myocytes. *Basic Res Cardiol* **88**: 93–102.

Wang QD, Pernow J, Sjöquist PO, Rydén L (2002). Pharmacological possibilities for protection against myocardial reperfusion injury. *Cardiovasc Res* **55**: 25–37.

Wu TS, Leu YL, Chan YY, Yu SM, Teng CM, Su JD (1994). Lignans and an aromatic acid from *Cinnamomum philippinense*. *Phytochemistry* **36**: 785–788.

Yu SM, Ko FN, Wu TS, Lee JY, Teng CM (1994a). Cinnamophilin, a novel thromboxane A_2 receptor antagonist, isolated from *Cinnamomum philippinense*. *Eur J Pharmacol* **256**: 85–91.

Yu SM, Wu TS, Teng CM (1994b). Pharmacological characterization of cinnamophilin, a novel dual inhibitor of thromboxane synthase and thromboxane A_2 receptor. *Br J Pharmacol* **111**: 906–912.